

# RSC Advances



This is an *Accepted Manuscript*, which has been through the Royal Society of Chemistry peer review process and has been accepted for publication.

*Accepted Manuscripts* are published online shortly after acceptance, before technical editing, formatting and proof reading. Using this free service, authors can make their results available to the community, in citable form, before we publish the edited article. This *Accepted Manuscript* will be replaced by the edited, formatted and paginated article as soon as this is available.

You can find more information about *Accepted Manuscripts* in the [Information for Authors](#).

Please note that technical editing may introduce minor changes to the text and/or graphics, which may alter content. The journal's standard [Terms & Conditions](#) and the [Ethical guidelines](#) still apply. In no event shall the Royal Society of Chemistry be held responsible for any errors or omissions in this *Accepted Manuscript* or any consequences arising from the use of any information it contains.

## ARTICLE

# Hierarchical carbon-nanotube/quartz-fiber films with gradient nanostructures for high efficiency and long service life air filters

Cite this: DOI: 10.1039/x0xx00000x

Received 00th January 2012,  
Accepted 00th January 2012

DOI: 10.1039/x0xx00000x

[www.rsc.org/](http://www.rsc.org/)

Peng Li,<sup>a,b,e</sup> Chunya Wang,<sup>a,b</sup> Zheng Li,<sup>c</sup> Yichen Zong,<sup>d</sup> Yingying Zhang,<sup>b,\*</sup> Xudong Yang,<sup>c</sup> Shuiqing Li<sup>d</sup> and Fei Wei<sup>a,b,\*</sup>

Hierarchical and gradient nanostructures are important to exploit the full potential of nanofibers in filtration applications. The introduction of gradient into carbon nanotube (CNT)/fiber hierarchical structure could result in a change of the particle capturing properties. Here we show the fabrication of hierarchical carbon nanotube (CNT)/quartz-fiber (QF) filters with gradient nanostructures where the content of CNTs decreases exponentially along the thickness direction of the filters. The loading of catalysts for the growth of CNTs in QF filter has been achieved through aerosol technique, which can be carried out in large-scale. With only 1.17 wt% CNT, the penetration of the CNT/QF filter at most penetrating particle size (MPPS) has been reduced by one order of magnitude, while the pressure drop only increases about 6% with respect to that of the pristine QF filter, leading to an obvious higher quality factor ( $Q_f$ ) of CNT/QF filters. More importantly, the service life of the CNT/QF filter with CNT-rich side downstream has increased by 64% compared with the pristine QF filter. In contrast, when CNT-rich side is placed upstream, the service life of CNT/QF filter will be only 41.7% of placing CNT-rich side downstream. Scanning electron microscope (SEM) images reveal that the gradient nanostructure of the CNT/QF filter and the CNT/QF hierarchical structure play very important roles in the simultaneous enhancement of the filtration efficiency and the service life of the air filters.

## Introduction

Air filtration is of primary importance in many fields such as cabin environment, nuclear industry, indoor environment, clean room and engine emission reduction. Fibrous filter is the most commonly used method to remove airborne particles with high efficiency, especially for particulate matters smaller than 1  $\mu\text{m}$ . Practical fibrous filters do not act as sieve because the sieve structure tends to be clogged quickly, resulting in excessively high pressure drop. In fact, fibrous filters usually have high porosity and the inter-fiber distances are larger than the size of particles. Aerosol particles are removed from gas flows mainly based on following mechanisms: direct interception, Brown diffusion and the forces of inertia, gravity, or electrical attraction. The first two ones predominate the filtration process of sub-micron aerosol particles.<sup>1-3</sup>

Filtration efficiency and pressure drop are two most important parameters of fibrous filters. They keep constant at the beginning phase of filtration. During the filtration process, aerosol particles will gradually accumulate at the fiber surface, causing the clogging of filter.<sup>4-7</sup> This results in the sharp increase of the pressure drop and changes in filtration efficiency. Due to the

“clogging effect”, filters have to be disposed when their pressure drop reach a certain value, resulting in a limited service life of air filter. Service life is also an important parameter of air filter, particularly in many special fields such as aircraft, nuclear power station, and semiconductor industry, where the replacement of air filters is very expensive. Numerous studies have been devoted to the filtration efficiency and the pressure drop of air filters. In contrast, the clogging effect remains to be poorly understood and reports on the structure design of extending the service life of air filters are very limited.<sup>8,9</sup>

Recently, nanofibers have gain great interests in air filtration.<sup>10-16</sup> Compared with microfibers, the most significant advantage of nanofibers is the high available specific surface area,<sup>17</sup> which will be helpful for promoting contact between aerosols and fibers. Besides, according to the classic filtration theory, when the diameter of fiber is comparable with the mean free path of air molecules (about 66 nm at ambient conditions), the flow around the single fiber will be “slip flow”, “transition flow” or even “free molecule flow”, which means the disturbance of fibers on the flow pattern will be very small or even negligible.<sup>18,19</sup> Therefore, air filters made of nanofibers will theoretically have a high efficiency as well as low pressure drop. Currently, the

most popular nanofibers used in air filtration are polymer nanofibers.<sup>10,11,20,21</sup> Compared with polymer nanofibers, CNTs have much smaller diameters, a much higher specific surface areas and much better mechanical properties.<sup>39-40</sup> These advantages make CNT a perfect candidate for air filtration. Recently there have been a few reports on the application of CNTs in air filtration.<sup>13, 22-29</sup> The commonly used strategies of fabricating CNT-based air filters including coating CNT films on microfiber filters<sup>13</sup> which provide mechanical support for CNT layer or using free-standing thin CNT films directly<sup>27-29</sup>. When nanofibers especially CNTs are used as filter media, a high filtration efficiency of the nanofiber-based air filter is always come with a high pressure drop and a short service life. This is because nanofibers are more inclined to have high packing density and the pores between nanofibers are usually too small for aerosol particles. During the air filtration process, the nanofiber-based air filter will be easily clogged, resulting in a rapid increase of the pressure drop. Besides, it is also difficult to fabricate nanofiber-based air filter in large-scale and maintain their high structural stability under the air force during air filtration.

A good filter should have a high filtration efficiency, a low pressure drop and a long service life. In previous work, we have fabricated a depth-type hierarchical CNT/quartz fiber (QF) filter through in-situ growth of CNTs on QF fibers, which showed a greatly enhanced filtration efficiency with a small pressure drop increase.<sup>23</sup> In this work, we further develop the hierarchical CNT/QF filter into the hierarchical CNT/QF filter with gradient nanostructures along the thickness direction. We have also developed a method to utilize the large scale fabrication of the CNT/QF filter with gradient nanostructure by aerosol technique. We found that the introduction of CNTs in QF filter could significantly increase the filtration efficiency of air filter. More importantly, the service life of CNT/QF filter was found to be extended by placing the CNT-rich side down stream. Conversely, the service life of CNT/QF filter will be greatly shorted when placing the CNT-rich side upstream.

## Experimental

### Materials

The QF filters with diameter of 150 mm were purchased from Membrane Solutions Inc., and used directly as the substrate for CNT growth.  $\text{Fe}(\text{NO}_3)_3 \cdot 9\text{H}_2\text{O}$  (purity > 99.99%) and  $\text{Al}(\text{NO}_3)_3 \cdot 9\text{H}_2\text{O}$  (purity > 99.99%) was purchased from Tianjin Damao chemical reagent factory, China. Bis(2-ethylhexyl) sebacate (DEHS, AR, purity > 97%) was purchased from Aladdin reagent Co., Ltd., China. NaCl (purity > 99.5%) was purchased from Modern Oriental Fine Chemistry Co., Ltd., China. High purity nitrogen ( $\text{N}_2$ , purity > 99.999%), argon (Ar, purity > 99.999%), hydrogen ( $\text{H}_2$ , purity > 99.999%) and ethylene ( $\text{C}_2\text{H}_4$ , purity > 99.5%) supplied from Beiwen Gas Co., Ltd., China were used as-received.

### Material synthesis

### CATALYST LOADING ON QF FILTERS USING AEROSOL TECHNIQUE.

Aerosol technique was used to load catalyst on the QF filter. Firstly, catalyst aerosols were generated by atomizing 0.01 g/ml  $\text{Fe}(\text{NO}_3)_3 \cdot 9\text{H}_2\text{O}$  and  $\text{Al}(\text{NO}_3)_3 \cdot 9\text{H}_2\text{O}$  (the molar ratio of  $\text{Fe}^{3+}:\text{Al}^{3+} = 0.8:1$ ) mixed aqueous solution using a constant output atomizer (model 3076, TSI). The concentration and particle size distribution of catalyst aerosols were shown in Fig. S1. Catalyst aerosol particles were dried by a diffusion drier and then passed through the QF filter with area of 100  $\text{cm}^2$  for 30 min,  $\text{N}_2$  was used as carrier gas and the gas flow rate was 0.22  $\text{cm}^3/\text{s}$ . The catalyst loading process was illustrated in Fig. S2.

**GROWTH OF CNTS ON QF FILTERS WITH GRADIENT NANOSTRUCTURES.** The growth of CNTs with gradient nanostructures upon QF filters was accomplished by chemical vapor deposition (CVD) method. Before the CVD process, the catalyst-loaded QF filter was annealed at 800  $^\circ\text{C}$  for 15 min in Ar (300  $\text{ml min}^{-1}$ ) flow. After that, a gas flow of Ar (300  $\text{ml min}^{-1}$ ),  $\text{H}_2$  (200  $\text{ml min}^{-1}$ ) and ethylene (200  $\text{ml min}^{-1}$ ) was introduced into a quartz tube (inner diameter 73 mm) from the beginning of the CVD process. The furnace was heated to 800  $^\circ\text{C}$  in 40 min and maintained for 60 min. Then the furnace was cooled down to room temperature in Ar (300  $\text{ml min}^{-1}$ ) and  $\text{H}_2$  (10  $\text{ml min}^{-1}$ ) atmosphere. The CNT/QF filters with area of 100  $\text{cm}^2$  were fabricated.

### Characterization of the materials

The morphology of the pristine QF filter and CNT/QF filter were characterized using a scanning electron microscope (SEM) (JSM 7401F) and a transmission electron microscope (TEM) (JEM 2010). Mercury intrusion porosimetry (for determining pore distributions in the filters) was performed using a Micromeritics AutoPore IV 9500 system (Micromeritics Corp., Norcross, GA). Brunauer Emmett Teller (BET) surface areas were determined by using Quadra Sorb Station (Quantachrome Instruments Corp., Florida, USA). Thermo gravimetric analysis (TGA) measurement was carried out on a thermo gravimetric analyzer instrument (TGA Q500) at a scan rate of 10  $^\circ\text{C}/\text{min}$  from 30 to 1000  $^\circ\text{C}$  in a  $\text{O}_2$  (50  $\text{ml min}^{-1}$ ) and  $\text{N}_2$  (20  $\text{ml min}^{-1}$ ) mixed flow.

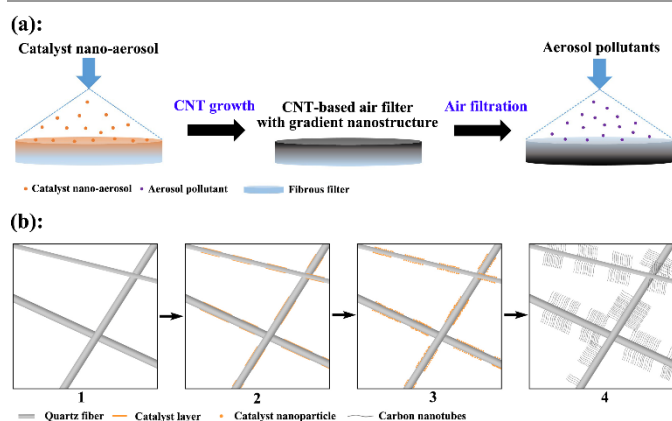
### Testing of filtration performance

To measure the filtration performance, the filter was placed into a filter holder with an inner area of 100  $\text{cm}^2$  at a face velocity of 5.31  $\text{cm}/\text{s}$ .  $\text{N}_2$  was used as carrier gas. Aerosols were generated by atomizing DEHS solution by using a constant output atomizer (model 3076, TSI) and operating in the recirculation mode. Aerosol particles were then dried by a diffusion drier. The aerosol concentration and size distribution at the upstream and downstream of the filter were measured by a scanning mobility particle sizer (SMPS, model 3936, TSI), which consists of an electrostatic classifier (model 3080, TSI) with a Long Differential Mobility (model 3081, TSI) and an ultracondensational particle counter (UCPC 3776 low, TSI). The pressure drop of the filters was measured by a pressure transmitter (P3000T, Bestace). A typical DEHS aerosol concentration and size distribution at the upstream was shown in Fig. S3. To measure the filtration performance changes of filters

under continuous aerosol loading, the concentration of aerosols was measured every 3 min and the pressure drop of filters was recorded every 30 seconds. At least three experiments were performed to ensure reproducibility of the results.

To measure the morphology of aerosols loading on the fiber surface of air filter, 0.1 g ml<sup>-1</sup> NaCl aqueous solution was atomized by a constant output atomizer (model 3076, TSI) and then dried by a diffusion drier. NaCl aerosols were carried by N<sub>2</sub> and passed through filters at a velocity of 9.18 cm/s for a period of 60 seconds and 6 min, respectively. A typical NaCl aerosol concentration and size distribution at the upstream was shown in Fig. S4.

## Results and discussion



Scheme 1: Synthesis process of the CNT/Quartz fiber filter. (a) Scheme illustrating the catalyst loading on Quartz fiber filter using aerosol technique and the growth of CNTs with its content decrease along the thickness of filter to form a CNT-based air filter with gradient nanostructure. The CNT-rich side will be putted downstream for air filtration. (b) Scheme further illustrate CNT growing process on QF filter. 1 stands for the pristine QF filter, 2 stands for catalyst layer formed on QFs after catalyst nano-aerosol filtrated by QF filter, 3 stands for catalyst nanoparticles formed on QFs after annealing, 4 stands for CNT growth on QF after CVD process.

Depositing catalysts on QFs in large-scale is the first step for the large-scale fabrication of CNT/QF filters. Although various methods of depositing catalysts on structured surfaces have been reported,<sup>30</sup> herein we have developed a facile method for depositing catalysts on porous structures, as shown in Scheme 1. According to the principles of air filtration, aerosol particles will be captured on the surface of fibers and their contents will decrease gradually in the filter along the direction of air flow (Scheme 1a). Therefore, if catalyst aerosols are filtrated by a fibrous filter, they will deposit on the fiber surface and form a thin layer around the fiber (Scheme 1b-2). After annealing, catalyst nanoparticles will form on the fiber surface (Scheme 1b-3). Then, CNTs can grow on the fiber surface after the CVD process (Scheme 1b-4). The CNT content will decrease gradually in the thickness direction of filter, which is in consistent with the concentration distribution of catalyst aerosols in filters (Scheme 1a). For air filtration, the CNT-rich side of the CNT/QF filter will be placed downstream to remove air pollutants.

Fig. 1 shows the process of CNTs grown on a QF filter and the morphologies of the CNT/QF filter. The pristine QF filter is

formed by randomly stacked QFs with diameters in the range of 0.3 ~ 5 μm. The typical macroporous structure can be seen in Fig. 1a. After catalyst aerosols are filtrated by QF filter, they will deposit on the surface of QFs and form thin layers (Fig. 1b). These catalyst layers are non-uniformly coated on QFs as indicated by black arrows (Fig. 1b), which can be seen more clearly in Fig. 1c, catalyst layers will transform into catalyst nanoparticles on QFs after annealing. The non-uniform coverage of catalyst nanoparticles on QFs can be attributed to the disturbance of the airflow by the nearby fibers. Therefore, catalyst nanoparticles can only partially contact with QFs. As a result, CNTs are grown bunchy on QFs since catalysts cover the QFs non-uniformly (Fig. 1d). The pristine QF filter has a high filtration efficiency and very few catalysts could penetrate through the filter. Therefore, there are very few catalysts deposited on the downstream side of QF filter. Consequently, on downstream side there are almost no CNTs grow (Fig. 1e). The CNTs synthesized in this work are multi-walled CNTs with diameters in the range of 10-30 nm (Fig. 1f).

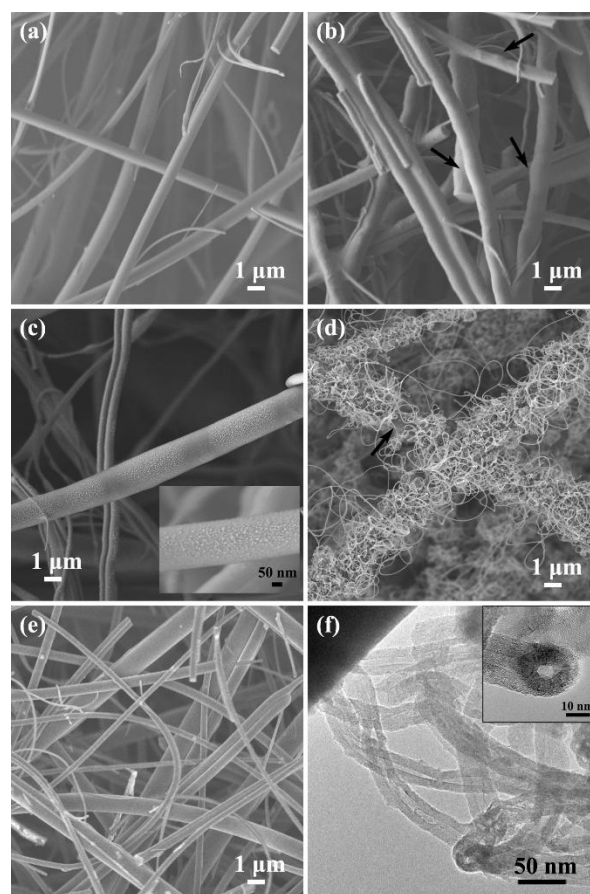


Fig. 1: SEM (a-e) and TEM (f) images of QF or CNT/QF filter. (a) the pristine QF filter; (b) QF filter with a deposited catalyst layer (as indicated by black arrows); (c) QF filter with a deposited catalyst layer after annealing (inset shows high-magnification SEM of catalyst nanoparticles); (d) the as-obtained CNT/QF filter (black arrow shows the part of fiber where no CNTs grow); (e) the side with almost no CNTs; (f) TEM image of the as-grown CNTs (inset shows high-magnification TEM of the end of CNTs).

The fabricated CNT/QF filter has gradient nanostructures, as shown in Fig. 2. The as-prepared CNT/QF filter can be divided into three separate layers along the thickness direction, which including the top layer (the upstream layer when catalyst loading), the middle layer and the bottom layer (Fig. 2a). Fig. 2b, Fig. 2d and Fig. 2f show the high-magnification SEM images of the up layer in Fig. 2a from top to bottom along the air flow direction. It can be found that the amount of CNTs in QF filter shows a sharp decrease in this direction (indicated by the red dash circle).

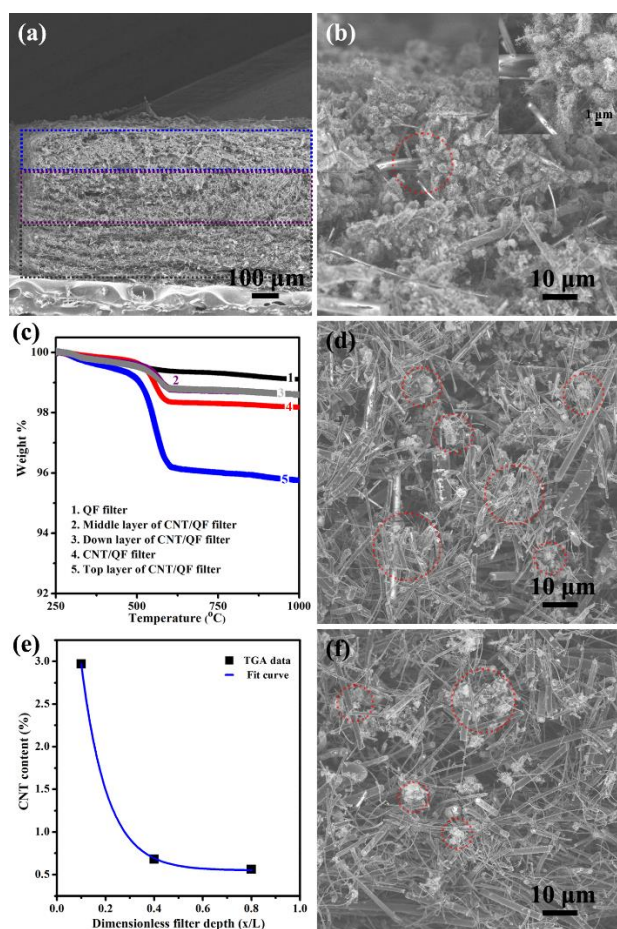


Fig. 2: SEM images of the cross-section of CNT/QF filter. (a) Low-magnification SEM of the cross-section of CNT/QF filter (the blue, purple and gray dashed box shows the top layer, the middle layer and the down layer of CNT/QF filter respectively); (b, d and f) high-magnification SEM of the up layer in Fig. (a) from top to bottom (the red dashed circle represents CNTs on QF fiber); (c) TGA traces of the pristine QF filter, CNT/QF filter, and the top, middle, down layer of CNT/QF filter; (e) exponential fit trace of CNT content of the top, middle, down layer of CNT/QF filter.

Thermo gravimetric analysis (TGA) measurement is used to study the content of CNTs in the CNT/QF filter and its distribution in each layer (Fig. 2c). Both CNT/QF filter and its different layers have a weight loss between 400 °C - 670 °C, which can be attributed to the decomposition of CNTs. The total content of CNTs in the CNT/QF filter is calculated to be 1.17%, while the CNT content in the top, middle and bottom layer is calculated to be 2.97%, 0.68% and 0.56%, respectively (Table 1). TGA results have confirmed that CNT/QF filters have gradient

nanostructures with CNT content decrease along the thickness direction. The growth of CNTs will mainly concentrated on the top layer of the QF filter, which is in the upstream side during catalyst loading. Brown et al<sup>31</sup> have derived an expression on the mass deposition profile of a homogeneous fibrous filter under continuous loading of monodisperse aerosols. They found the concentration of deposited aerosols exponentially decreased along the thickness direction from upstream layer to downstream layer for a non-clogging filter. In this work, the pristine QF filter can be considered as a homogeneous fibrous filter. During the catalyst depositing process, the concentration of catalyst aerosols and the velocity of carry gas are kept at a low level so that the clogging of QF filter is avoided. This can also be confirmed in Fig. 1b, where catalyst aerosols only form thin layers around QF rather than porous thick layer on the filter surface. Therefore, Brown's expression can be applied to estimate the catalyst deposition profile of the QF filter in spite of polydisperse catalyst aerosols used in this work.<sup>8, 9</sup> The concentration of catalyst is decrease exponentially along the thickness direction, which will result in the exponential decrease of CNT content in the same direction, as shown in Fig. 2e.

Table 1: Comparison of the structure properties and filtration performance of a QF filter and a CNT/QF filter.

	QF filter	CNT/QF filter
		2.97 (up layer)
CNT content (wt %)	0	1.17 (Total)
		0.68 (middle layer)
		0.56 (down layer)
Thickness (mm)	0.37	0.43
Density (g/cm <sup>3</sup> )	0.22	0.20
Porosity (%)	90	90.1
Filter specific area (m <sup>2</sup> /m <sup>3</sup> )	$5.3 \times 10^5$	$8.6 \times 10^5$
Pressure drop (Pa) at 5.31 cm/s	407	435
Penetration at MPPS (MPPS)	$2.45 \times 10^{-4}$ (88.2 nm)	$4.13 \times 10^{-5}$ (63.8 nm)
$Q_f$ for MPPS (KPa <sup>-1</sup> )	20.43	23.21

The structure properties and filtration performance of the QF filter and the CNT/QF filter are summarized in Table 1. The penetration at the most penetrating particle size (MPPS) of the CNT/QF filter is reduced by nearly one order of magnitude compared with the QF filter, which indicates an obviously higher filtration efficiency of the CNT/QF filter than the QF filter. Besides, the MPPS of the filter has decreased from 88.2 nm to 63.8 nm after CNTs have grown on QF filter. The shift of MPPS towards smaller particles can be attributed to the enhancement of diffusion mechanism due to the introduction of CNTs.<sup>12</sup> At the same time, the pressure drop of the CNT/QF filter has only increased by 6.9% compared with the QF filter. The quality

factor ( $Q_f$ ) is usually taken as the criterion for comparing filtration performance of filters, which is expressed by

$$Q_f = \frac{-\ln P}{\Delta p}$$

where  $P$  is the penetration and  $\Delta p$  is the pressure drop of air filters. According to the classical filtration theory, a higher  $Q_f$  stands for a better performance of the filter.<sup>2</sup> The CNT/QF filter have much higher  $Q_f$  than the QF filter in all the particle size tested (Fig. S5), which indicates the deposition of CNTs on QF has enhanced the filtration performance of the raw filter. This is consistent with the result we have reported before.<sup>23</sup> The role of CNTs in improving filtration efficiency and the dust holding capacity of the raw filters has been investigated by SEM and the results are shown in Fig. S6.

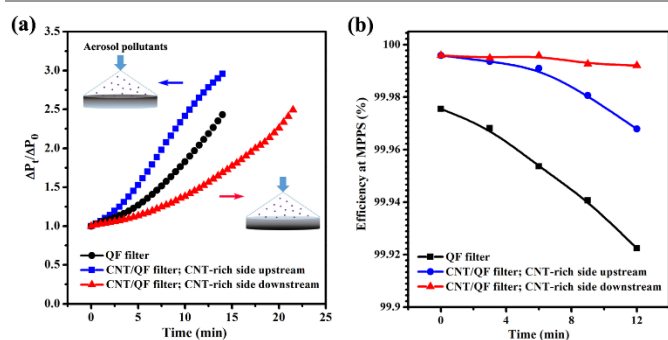


Fig. 3: (a) Pressure drop increase rate versus filtration test time of CNT/QF filter with different way of placement and QF filter under continuous aerosol loading; (b) decrease rate of efficiency at MPPS versus filtration test time of CNT/QF filter with different way of placement and QF filter under continuous aerosol loading.

The dynamic filtration processes of the CNT/QF filter and the QF filter are shown in Fig. 3. Since DEHS aerosols are liquid aerosols, the filtration of liquid aerosols by oleophilic fibrous filters under continuous aerosol loading can be divided into four separate steps.<sup>32, 33</sup> During the first step, the filter will be wetted by deposited liquid particles and a thin film will form around the fiber. This film has very little interference on the airflow. However, it will reduce the fiber collection area. As a result, the pressure drop will increase slowly whereas the penetration will increase rapidly.<sup>6</sup> As liquid aerosols continue to accumulate on fiber surface, the filtration will enter into the second step. This aerosol film will be broken up due to the Plateau-Rayleigh instability<sup>34, 35</sup> and droplets will form on the fiber surface. These droplets can further coalesce to form bigger drops and bridges between fibers,<sup>36</sup> leading to an exponential increase of penetration, which can also be attributed to the decrease in fiber collection area. The pressure drop will increase rapidly in this step. In the third stage, the interstices between fibers will be occupied by large drops in a short time, which results in a massive increase of pressure drop. At the same time, the gas interstitial velocity will increase and contribute to a diminution of the penetration by enhanced impaction collection.<sup>4</sup> At the end of clogging, the filter will reach an equilibrium state. In this stage, a pseudo-stationary state is established between collection and

drainage of liquid droplets. The pressure drop and filter penetration will be constant.

Both the QF filter and the CNT/QF filter can be well wetted by DEHS droplets (Fig. S7), so their dynamic filtration processes are in compliance with the above rules, as shown in Fig. 3a and 3b. The pressure drop of the QF filter and the CNT/QF filter has a significant increment under continuous aerosol loading during the filtration test (Fig. 3a). At the same time, the filtration efficiency decreases with test time (Fig. 3b). These characteristics suggest that the filtration test is undergoing the first and second step of the dynamic filtration process. It is founded that the CNT/QF filter with CNT-rich side downstream have an obviously slower pressure drop rise than the QF filter (Fig. 3a). Although the evaluation of the service life of air filter is a challenging problem due to the changing external environment and the influence of environmental factors on filter loading such as aerosol concentration, particle size distribution, and temperature and so on,<sup>10</sup> it is generally recommended that HEPA filters (high efficiency particulate air filter with efficiency higher than 99.97% at MPPS) should be replaced when the pressure drop reaches twice of their initial value.<sup>37</sup> Therefore, in this work we use the time required when the filter pressure drop reach two times of the initial value to evaluate the service life of each filter, the detail information is shown in Table S1. For the QF filter, the service life is only 11 min due to the high concentration of testing aerosols used in this work, while for the CNT/QF filter with CNT-rich side downstream, the service life is 18 min, which is 1.64 times of the QF filter. However, if CNT-rich side is placed upstream, the pressure drop of the CNT/QF filter will increase very quickly and the service life is only 7.5 min. The different placement direction of the CNT/QF filter will result in a 2.4 times difference in its service life.

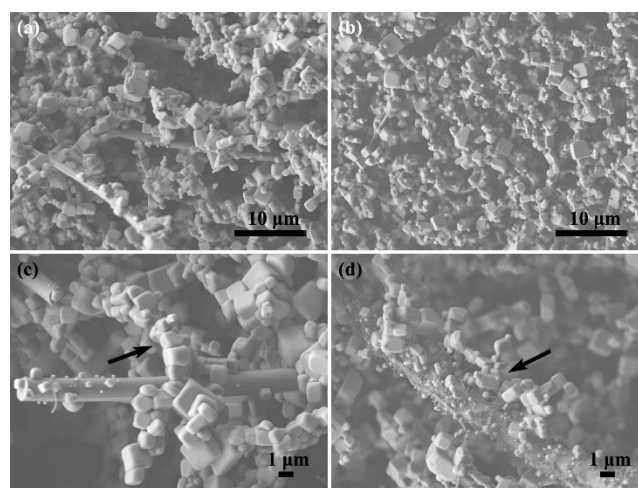


Fig. 4: SEM images of the filters with NaCl aerosol particles depositing for 6 min. (a) NaCl aerosol particles deposited on the surface of QF filter; (b) NaCl aerosol particles deposited on the surface of CNT/QF filter; (c) NaCl aerosol particles accumulated on signal QF fiber (the black arrow shows large aerosol particle aggregates formed on signal QF fiber); (d) NaCl aerosol particles accumulated on an isolated CNT/QF fiber (the black arrow shows small aerosol particle aggregates formed on an isolated CNT/QF fiber).

At the same time, it is founded that the filtration efficiency of the QF filter has a sharp decline under continuous aerosol loading. It no longer meets the standard of HEPA filters very quickly (Fig. 3b). In contrast, the filtration efficiency of the CNT/QF filter with CNT-rich side downstream remains at a very high level that above the standards of HEPA filter, as shown in Table S1. If the CNT-rich side is placed upstream, the decrease of filtration efficiency of the CNT/QF filter will become faster, but still lower than that of the QF filter. Therefore, we can concluded that the CNT/QF filter with CNT-rich side downstream is a much better air filter than the CNT/QF filter with CNT-rich side upstream, even if they have the same filtration performance and  $Q_f$  at the initial stage of air filtration. Compared with the filtration performance of the pure QF filter and the CNT/QF filter, we can further conclude that the filter with a higher  $Q_f$  is not an absolutely better filter since it may have a much shorter service life. The evaluation of filter performance should be based on both the  $Q_f$  of filters at initial filtration stage and the service life.

NaCl aerosols are used to study the loading behaviour of the QF filter and CNT/QF filter, since DEHS aerosols are not suitable for SEM observation. The results are shown in Fig. 4. From Fig. 4a and Fig. 4b, it can be found that there are much more NaCl aerosols deposited on the filter surface when the CNT-rich side is placed upstream. This proves that when high filtration efficiency layer is placed upstream, the filter are easier to be clogged. It is noteworthy that there is a trend to fabricate air filters through coating a nanofiber layer on the surface of macrofiber layers.<sup>10, 13, 38</sup> However, this is not a rational structure since the nanofiber layer will accelerate the “clogging effect” and reduce the service life of filter, even if it will improve the filtration efficiency and  $Q_f$  at the initial state. When aerosols are continuous depositing on QF (Fig. 4c), they will accumulate into large aggregates and clog pores between fibers (indicated by black arrow). However, when CNTs are grown on QFs (Fig. 4d), aerosol aggregates will be much smaller (indicated by black arrow), since CNTs have high specific surface area for aerosol loading. As a result, the resistance to air flow will be also smaller. This explains why the CNT/QF filter with CNT-rich side downstream has a much higher service life than the QF filter.

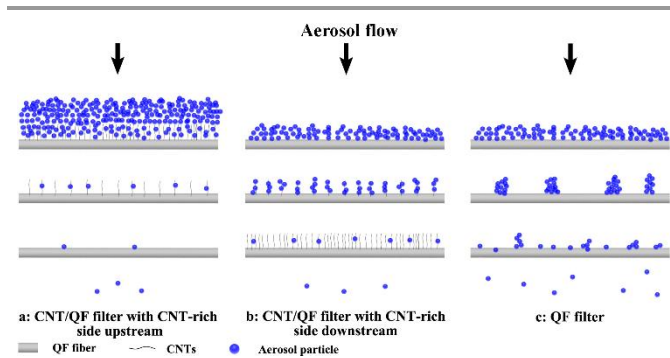


Fig. 5: illustration of aerosols accumulating in CNT/QF filter with different way of placement and QF filter.

Based on the above results, it can be seen that the growth of CNTs with gradient distribution is very important for the

performance of the CNT/QF filter, which combines high filtration efficiency, high  $Q_f$ , and high service life. The influence of CNTs and the structure arrangement on the filtration performance can be illustrated in Fig. 5. For the CNT/QF filter, CNTs are grown with gradient structure in QF filter. If the CNT-rich side is placed upstream (Fig. 5a), the surface layer will have a high filtration efficiency and the majority of DEHS aerosols will be trapped on the surface of filter. As a result, the “clogging effect” will be accelerated. In this work, DEHS aerosols will form large drops on the fiber surface very quickly, resulting in a rapid increase of pressure drop and decrease of filtration efficiency. On the contrary, if the CNT-rich side is placed downstream (Fig. 5b), the upstream layer has a low filtration efficiency and there will be much less DEHS aerosols trapped on the surface of filter. Thus, the “clogging process” will be slowed down. The rest of aerosols which have penetrated through the surface layer will be removed by the CNT-rich layer with a high efficiency. At the same time, the rest of aerosols which have penetrated through the upstream layer have a very limited concentration. Therefore, their clogging effects to the CNT-rich layer will be drastically weakened. Therefore, the CNT/QF filter with CNT-rich side downstream will have a high efficiency and a high service life simultaneously. Compared with the QF filter (Fig. 5c), the advantage of the CNT/QF filter with CNT-rich side downstream lies in the high specific surface area of CNTs. Therefore, the rapid formation of large aerosol aggregates or drops which occupy the voids between fibers will be avoided. As a result, the increase of pressure drop and the decrease of filtration efficiency of the CNT/QF filter will be slower than the QF filter.

## Conclusions

In summary, hierarchical CNT/QF filters with gradient nanostructures have been fabricated with the assistance of aerosol technique. Compared with the pristine QF filter, the CNT/QF filter has significantly improved filtration efficiency and an obviously higher  $Q_f$ . Furthermore, the CNT/QF filter with CNT-rich side downstream shows a dramatically longer service life than the QF filter. We also found that when the CNT-rich side was placed upstream, the service life will be greatly shortened. Although the CNT/QF filter showed same filtration performance at the clean state when being placed in an opposite direction, their performances during the dynamic filtration process are obviously different. This study provides a new strategy for the fabrication of high performance air filters through taking advantages of each structure unit in a hierarchical structure, which includes microfibers with high structure stability and CNTs with high specific surface area, combing the high dust holding capacity of the upstream QF layer and the high filtration efficiency of the downstream CNT-rich layer.

## Acknowledgements

The work is supported by the Boeing Company and the National Science Foundation of China (21203107), National Natural

Science Funds of China (50976058), National Key Basic Research and Development Program (2013CB228506).

## Notes and references

<sup>a</sup> Beijing Key Laboratory of Green Chemical Reaction Engineering and Technology, Department of Chemical Engineering, Tsinghua University, Beijing, 100084, China. E-mail: wf-dce@tsinghua.edu.cn

<sup>b</sup> Center for Nano and Micro Mechanics, Tsinghua University, Beijing, 100084, China. E-mail: yingyingzhang@tsinghua.edu.cn

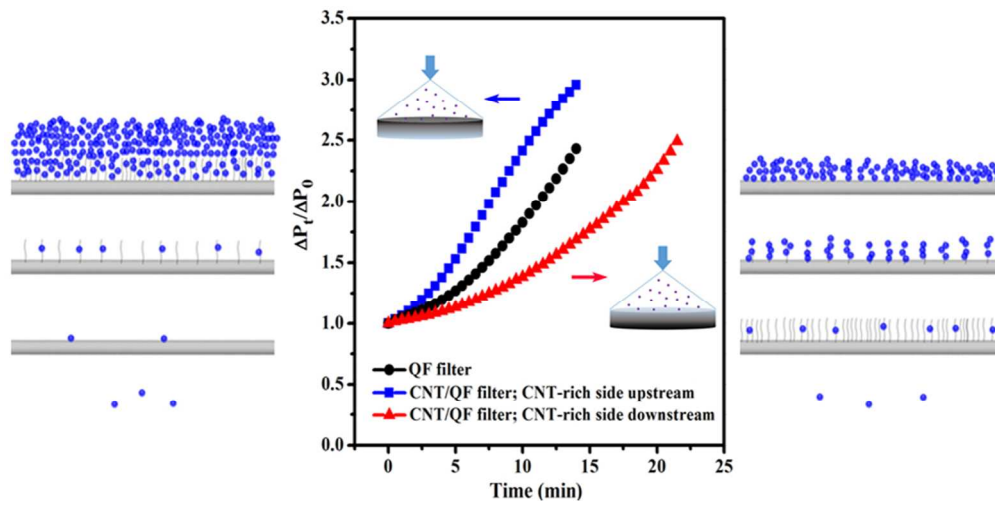
<sup>c</sup> Department of Building Science, Tsinghua University, Beijing, 100084, China.

<sup>d</sup> Key Laboratory for Thermal Science and Power Engineering of Ministry of Education, Tsinghua University, Beijing, 100084, China.

<sup>e</sup> Jibe Electric Power Research Institute, State Grid Jibe Electric Power Company Limited, Beijing, 100045, China.

† Electronic Supplementary Information (ESI) available: [Typical size distribution of atomized catalyst aerosols used for catalyst loading on QF filters; the schematic of the catalyst loading process of QF filter and the digital photo of as-prepared CNT/QF filter; typical size distribution of atomized polydisperse DEHS aerosols used for air filtration test; typical size distribution of atomized polydisperse NaCl aerosols used for loading on the CNT/QF filters and QF filters; the filtration performance of the QF filter and the CNT/QF filter; SEM images of the filters with NaCl aerosol particles depositing for 60 seconds; the contact angles test of DEHS droplets on a QF filter and a CNT/QF filter]. See DOI: 10.1039/b000000x/

- R. C. Brown, *Air filtration: an integrated approach to the theory and applications of fibrous filters*, Pergamon press Oxford, England, 1993.
- C. Y. Chen, *Chem. Rev.*, 1955, **55**, 595-623.
- C. N. Davies, *Air filtration*, Academic press London, 1973.
- P. Contal, J. Simao, D. Thomas, T. Frising, S. Callé J. C. Appert-Collin and D. Bémer, *J. Aerosol Sci.*, 2004, **35**, 263-278.
- C. B. Song, H. S. Park and K. W. Lee, *Powder Technol.*, 2006, **163**, 152-159.
- D. C. Walsh, J. I. T. Stenhouse, K. L. Scurrah and A. Graef, *J. Aerosol Sci.*, 1996, **27**, Supplement 1, S617-S618.
- S. Payet, D. Boulaud, G. Madelaine and A. Renoux, *J. Aerosol Sci.*, 1992, **23**, 723-735.
- W. W.-F. Leung and C.-H. Hung, *Sep. Purif. Technol.*, 2012, **92**, 174-180.
- W. W.-F. Leung, C.-H. Hung and P.-T. Yuen, *Aerosol Sci. Technol.*, 2009, **43**, 1174-1183.
- K. Graham, M. Ouyang, T. Raether, T. Grafe, B. McDonald and P. Knäuf, *Polymeric nanofibers in air filtration applications*, 2002.
- H. Misslitz, K. Kreger and H.-W. Schmidt, *Small*, 2013, **9**, 2025-2025.
- A. Podgórski, A. Bałazy and L. Gradoń, *Chem. Eng. Sci.*, 2006, **61**, 6804-6815.
- G. Viswanathan, D. B. Kane and P. J. Lipowicz, *Adv. Mater.*, 2004, **16**, 2045-2049.
- O. Yildiz and P. D. Bradford, *Carbon* 2013, **64**, 295-304.
- R. Balamurugan, S. Sundarrajan and S. Ramakrishna, *Membranes*, 2011, **1**, 232-248.
- R. S. Barhate and S. Ramakrishna, *J. Membr. Sci.*, 2007, **296**, 1-8.
- P. Gibson, H. Schreuder-Gibson and D. Rivin, *Colloids Surf., A*, 2001, **187-188**, 469-481.
- B. Maze, H. Vahedi Tafreshi, Q. Wang and B. Pourdeyhimi, *J. Aerosol Sci.*, 2007, **38**, 550-571.
- Z. Zhang, Ph.D. Thesis, University of Minnesota, 1989.
- Y. Ahn, S. Park, G. Kim, Y. Hwang, C. Lee, H. Shin and J. Lee, *Curr. Appl. Phys.*, 2006, **6**, 1030-1035.
- N. Wang, X. Wang, B. Ding, J. Yu and G. Sun, *J. Mater. Chem.*, 2012, **22**, 1445-1452.
- N. Halonen, A. Rautio, A.-R. Leino, T. Kyllonen, G. Toth, J. Lappalainen, K. Kordás, M. Huuhtanen, R. L. Keiski and A. Sági, *ACS Nano*, 2010, **4**, 2003-2008.
- P. Li, Y. Zong, Y. Zhang, M. Yang, R. Zhang, S. Li and F. Wei, *Nanoscale*, 2013, **5**, 3367-3372.
- A. G. Nasibulin, A. Kaskela, K. Mustonen, A. S. Anisimov, V. Ruiz, S. Kivisto, S. Rackauskas, M. Y. Timmermans, M. Pudas and B. Aitchison, *ACS Nano*, 2011, **5**, 3214-3221.
- H. Parham, S. Bates, Y. Xia and Y. Zhu, *Carbon*, 2013, **54**, 215-223.
- J. H. Park, K. Y. Yoon, H. Na, Y. S. Kim, J. Hwang, J. Kim and Y. H. Yoon, *Sci. Total Environ.*, 2011, **409**, 4132-4138.
- S. J. Park and D. G. Lee, *Carbon*, 2006, **44**, 1930-1935.
- S. J. Park and D. G. Lee, *Curr. Appl. Phys.*, 2006, **6**, e182-e186.
- O. Yildiz and P. D. Bradford, *Carbon*, 2013, **64**, 295-304.
- V. Meille, *Appl. Catal., A*, 2006, **315**, 1-17.
- R. C. Brown and D. Wake, *J. Aerosol Sci.*, 1999, **30**, 227-234.
- T. Frising, D. Thomas, D. Bémer and P. Contal, *Chem. Eng. Sci.*, 2005, **60**, 2751-2762.
- A. Bredin and B. J. Mullins, *Sep. Purif. Technol.*, 2012, **90**, 53-63.
- B. J. Mullins and G. Kasper, *Chem. Eng. Sci.*, 2006, **61**, 6223-6227.
- R.-J. Roe, *J. Colloid Interface Sci.*, 1975, **50**, 70-79.
- P. C. Raynor and D. Leith, *J. Aerosol Sci.*, 2000, **31**, 19-34.
- Z. Xu, *Fundamentals of air cleaning technology and its application in cleanrooms*, Springer, 2014.
- D. Cho, A. Naydich, M. W. Frey and Y. L. Joo, *Polymer*, 2013, **54**, 2364-2372.
- X. Li, J. Yang, Y. Hu, J. Wang, Y. Li, M. Cai, R. Li and X. Sun, *J. Mater. Chem.*, 2012, **22**, 18847-18853.
- Q. Zhang, J. Q. Huang, W. Z. Qian, Y. Y. Zhang and F. Wei, *Small*, 2013, **9**, 1237-1265.



80x39mm (300 x 300 DPI)

"Gradient nano-structure filtration" for the simultaneous enhancement of the filtration efficiency and the service life of air filters.